e-ISSN 2580 - 0752

BULLETIN OF
GEOLOGY
Fakultas Ilmu dan Teknologi Kebumian (FITB)
Institut Teknologi Bandung (ITB)

MIDDLE MIOCENE BIOSTRATIGRAPHY AND PALEO-OCEANOGRAPHY OF SUPIORI ISLAND, PAPUA, BASED ON CALCAREOUS NANNOFOSSIL ASSEMBLAGES

RYAN DWI WAHYU ARDI[1,3], NADILA NOVANDARU[1], ISTIANA[1], ALVIYANDA[1,4], RUBIYANTO KAPID[1,] G.M. LUCKI JUNURSYAH[2], RAHMAT Y. SARAGIH[2]

[1]Geological Engineering Study Program, Institut Teknologi Bandung, Jl. Ganesha no. 10 Bandung 40132. Email: dwa.ryan@gmail.com.
[2]Geological Research Centre, Jl. Diponegoro no. 57 Bandung 40122
[3]Agrotechnology Study Program, Universitas Nahdlatul Ulama Purwokerto, Jl. Sultan Agung no. 42 Purwokerto 53144
[4]Geological Engineering Study Program, Institut Teknologi Sumatera, Jl. Terusan Ryacudu, Way Hui, Jati Agung, Lampung Selatan 25365

Sari - Kumpulan nanofosil gampingan dari tiga penampang stratigrafi di Pulau Supiori, Papua, telah dianalisis untuk memperoleh pembagian biozonasi dan kondisi paleo-oseanografinya. Berdasarkan Zonasi Nanofosil Gampingan Neogen (Martini, 1971), lintasan BK 78 (Formasi Wainukendi) terbagi menjadi tiga zona yang setara NN7 – NN9 (Miosen Tengah), lintasan BK 98 (Formasi Wafordori) setara dengan NN7 (Miosen Tengah), dan lintasan BK 95 (Formasi Napisendi) terbagi menjadi lima zona yang setara NN5–NN9 (Miosen Tengah). Hasil tersebut menunjukkan bahwa kemungkinan Formasi Wainukendi, Wafordori, dan Napisendi memiliki hubungan yang menjemari. Pada penelitian ini dilakukan pula analisis parameter paleo-oseanografi berupa kedalaman termoklin/nutriklin dan paleosalinitas. Analisis kedalaman termoklin/nutriklin, berdasarkan kelimpahan Discoaster dan ukuran rata-rata coccolith Reticulofenestra dan Coccolithus, menunjukkan perubahan dari kondisi oligotropik (NN5–NN7) menuju eutropik (awal NN8), kemudian kembali menjadi oligotropik sejak akhir NN8 hingga NN9. Analisis paleosalinitas berdasarkan perbandingan kelimpahan Sphenolithus neoabies, Helicosphaera carteri, dan Calcidiscus leptoporus menunjukkan perubahan kondisi dari salinitas normal (Zona NN7) menjadi hiposalin (Zona NN8–NN9). Perubahan parameter-parameter paleo-oseanografi tersebut kemungkinan berhubungan dengan penutupan jalur laut Kepulauan Indonesia akibat pengangkatan regional yang menyebabkan terbentuknya proto West Pacific Warm Pool (WPWP) dan Equatorial Under Current (EUC) sehingga terjadi kondisi serupa La Niña pada akhir Miosen Tengah (setara NN8–NN9).

Kata kunci: Ekuatorial Pasifik Barat, Nanofosil gampingan, Paleo-oseanografi, Paleosalinitas, Pulau Supiori, Termoklin/Nutriklin

Abstract- *Calcareous nannofossil assemblages have been analysed from three stratigraphic sections on Supiori Island to determine biozonation and paleo-oceanographic condition. Based on Neogene Calcareous Nannofossils Zonation (Martini, 1971), section BK 78 (Wainukendi Formation) classified into three zones, which coeval to NN7–NN9 and or younger (Middle Miocene). Section BK 95 (Napisendi Formation) categorised into five zones, which equivalent to NN5–NN9 (Middle Miocene), and section BK 98 (Wafordori Formation) is considered to be equivalent to NN7 (Middle Miocene). Those results indicate a correlatable interval (NN7) and an interfinger contact between Wainukendi, Wafordori, and Napisendi Formations. Paleo-oceanographic parameters namely thermocline/nutricline depth and paleosalinity were analysed in this research. Thermocline/nutricline depth analysis from Discoaster abundance and mean coccolith size of Reticulofenestra and Coccolithus indicate sea surface condition changes from oligotrophic (NN5–NN7) to eutrophic (early NN8) and then again into oligotrophic (from late NN8 to NN9). Paleosalinity analysis based on abundance comparison between Sphenolithus neoabies, Helicosphaera carteri, and Calcidiscus leptoporus denotes paleosalinity shift from normal saline (NN7) to hyposaline condition (NN8 – NN9). Those paleo-oceanographic parameters changes most likely related to the closing of Indonesian Seaway due to regional uplift, which triggered the formation of proto West Pacific Warm Pool (WPWP), Equatorial Under Current (EUC), and eventually a La Nina-like condition on late Middle Miocene (NN8–NN9).*

Keywords: *Calcareous nannofossil, Paleo-oceanography, Paleosalinity, Supiori Island, Thermocline/Nutricline, Western Equatorial Pacific*

DOI: 10.5614/bull.geol.2019.3.3.4

1. INTRODUCTION

Calcareous nannofossil has been known for its role on biostratigraphy, especially for lithological units aged less than 225 million years ago (Mya), where nannofossils is considered as high-resolution biostratigraphic markers. The mean age interval of nannofossil zones are 2 million years, some might longer (3 million years on Oligocene) or shorter (*Emiliana huxleyi* Zone : 200.000 years ago–Recent (Beggren et al., 1995). Furthermore, calcareous nannofossils are also considered as a good proxy to detect important paleobiological, paleoclimatical, and paleogeographical events, such as Trias/Jura extinction, Late Cretaceous maximum abundance, and Cretaceous/Tertiary planktonic extinction (Melinte, 2004).

This reseach will be focused on observing calcareous nannofossil specimens collected from stratigraphic sections BK 95, BK 98, and BK 78, outcropped on Supiori Island, Papua (**Figure 1**). These observation results then used for biostratigraphical analysis, to determine time relation between lithological units of the three stratigraphical sections, based on Martini (1971). In addition, paleo-oceanographic analysis is also inferred from the calcareous nannofossil assemblages, due to the location of the research area, near the West Pacific Warm Pool (WPWP). WPWP is the warmest ocean water mass, which has a great influence on the Intertropical Convergence Zone (ITCZ), Asian monsoon system and the famous *El Nino* Southern Oscillation (ENSO) (Sagawa, et al., 2012). These phenomena are the major regional and even global climatic-oceanographic drivers at Indo-Pacific Region (Martinez et al., 1998; Steinke et al., 2014). This paleo-oceanographic analysis will be focused on the possibility of early WPWP (proto WPWP) formation, during Middle Miocene, which is earlier than the estimation made by Nathan and Leckie (2009) (Late Miocene).

Geologically, from the stratigraphic, tectonic, and magmatic point of views, West New Guinea (Papua and West Papua Province, Indonesian) can be divided into three east-trending zones: Oceanic Zone (ophiolite and volcanic arc), Transition Zone (regionally strong-deformed metamorphic rocks), and Continental Zone (sediments over relatively stable basement) (Pieters et al., 1983) (**Figure 2**). These zones inferred tectonic history of this region, which strongly related to the convergence interaction between Caroline-Pacific Plate and Indo-Australian Plate. This convergence interaction was evolved from subduction to collision (Late Cretaceous), and finally into oblique convergence (Late Miocene), which triggered the formation of Sorong-Bewani-Yapen Strike-Slip Fault System (Waschmut and Kunst, 1986; McAdoo and Haebig, 2000). The subduction between Caroline-Pacific Plate and Indo-Australian Plate formed a hybrid forearc basin, known as North Irian Basin, which has strongly deformed since the Late Miocene (McAdoo and Haebig, 2000). This basin consists of several sub-basins such as Biak, Waropen, Waipoga, and Northeast Irian sub-basins (Pertamina, 1999 in McAdoo and Haebig, 2000).

DOI: 10.5614/bull.geol.2019.3.3.4

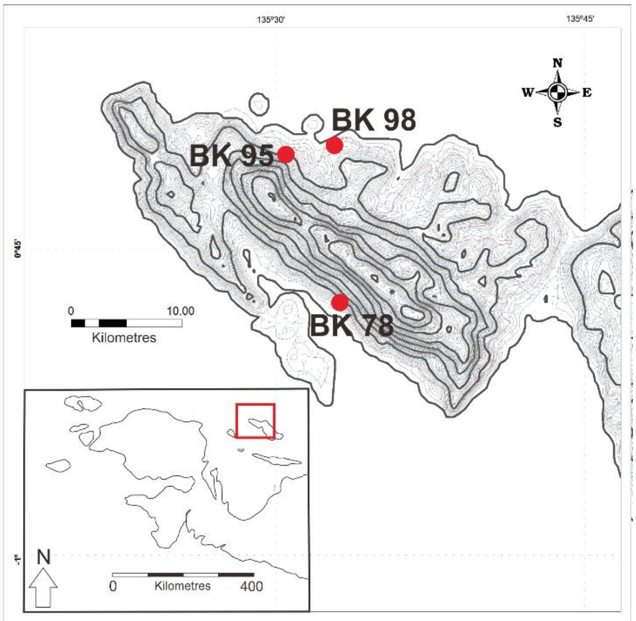

Figure 1. Research area (Supiori Island) and location of the stratigraphic sections (Junursyah et al., 2017).

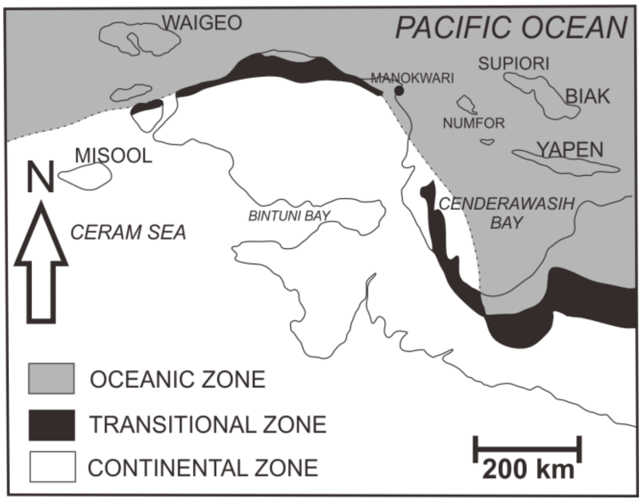

Figure 2.Geological zones of West New Guinea (modified from Pieters et al., 1983).

Supiori Island is considered as a part of North Irian Basin. This interpretation is based on the occurrence of Auwewa Formation, which considered as the product of the old island arc, and Korido metamorphic rocks, which considered as the oceanic basement (Pieters et al., 1983; Permana, 2015). Auwewa Formation is overlaid by the interfingering Wainukendi Formation (Oligocene–Middle Miocene), Wafordori Formation (Early–Middle Miocene) and Napisendi Formation (Early–Middle Miocene) (Pieters et al., 1983) (**Figure 3**).

DOI: 10.5614/bull.geol.2019.3.3.4

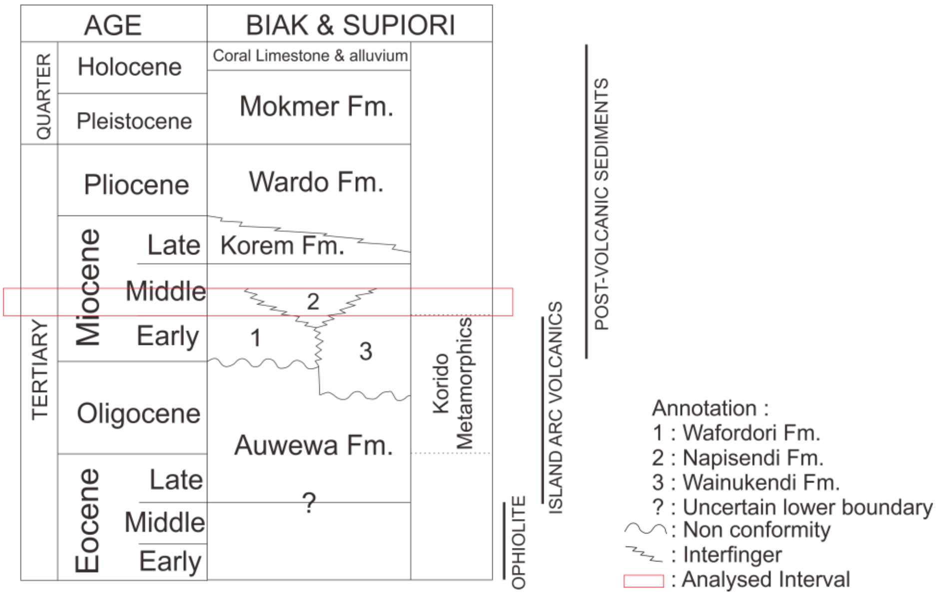

Figure 3. Regional stratigraphy of Biak and Supiori Island (modified from Pieters et al., 1983).

2. MATERIAL AND METHODS

2.1 Lithology

This research used sedimentary rock sample, which was taken from 3 stratigraphic sections: BK 78 (16,4 metres long), BK 98 (7,35 metres long), and BK 95 sections (32 metres long) (Junursyah et al., 2017; Alviyanda et. al., 2019). BK 98 consist of interbedded calcareous sandstone-calcareous claystone with mollusc and coral fragments. BK 95 consist of interbedded calcareous sandstone and calcareous siltstone with mollusc fragments and shelled organisms body in several parts. BK 78 consist of calcareous siltstone intercalated by calcareous sandstone and limestone on the bottom and interbedded limestone (wackestone and crystalline limestone) on the top generally with shelled organisms body, mollusc and coral fragments. Twenty (20) samples were collected from these sections with 3 m intervals. In detail, there are 3 samples collected from BK 98, 6 samples from BK 78, and 11 samples from BK 95.

2.2 Methods

The samples were prepared by spreading its hydrogen peroxide-soaked little part (~1 gram) on the slides, smearing the canada balsam on top of the slides, and finally putting the cover glass on top (smear slide method). Each slide was observed using Nikon YSH-2 polarized microscope. Calcareous nannofossils on each slide were then determined quantitatively. Two to three fields of view (fov) were counted for abundant samples and 10-12 fov for non-abundant samples from a total of 120 fov on each slide. Furthermore, coccolith diameters were measured from 100 *Reticulofenestra* sp. and *Coccolithus* sp. specimens on each sample. Calcareous nannofossils determinations were carried out based on Martini (1971), Perch-Nielsen (1985), and mikrotax.org, while the biozonation was determined according to Martini (1971).

Two paleo-oceanographic parameters, thermocline/nutricline depth and paleosalinity, were analysed. Thermocline/nutricline depths were inferred from the mean abundances of coccolith size (diameters) and percentages of the genus *Discoaster* (Farida et al., 2012; Imai et al., 2015; Pratiwi and Sato, 2016; Jatiningrum and Sato, 2017). However, the *Nannofossil Accumulation Rates* (NAR) weren't measured due to the unavailability of radiometric dating and dry weight measurements data. Paleosalinity was reflected rom the abundances of *Sphenolithus neoabies*, *Helicosphaera carteri*, and *Calcidiscus leptoporus* (Santoso et al., 2014). Summarized research methods shown in **Figure 4.**

DOI: 10.5614/bull.geol.2019.3.3.4

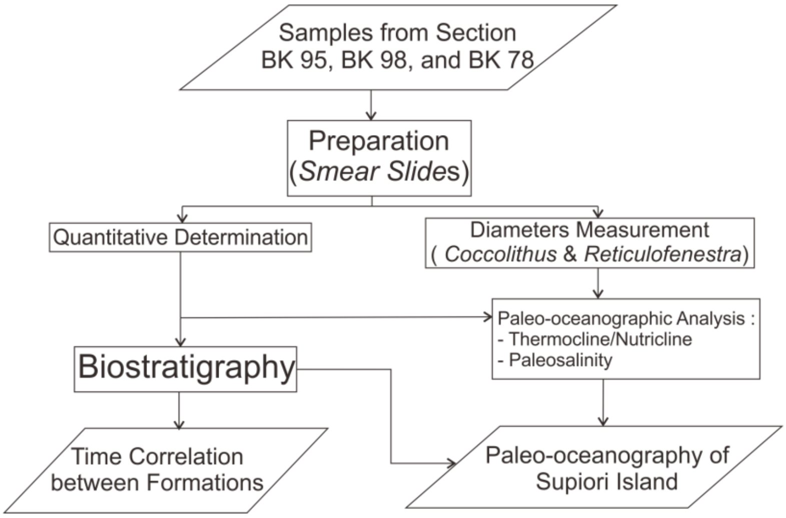

Figure 4. Summarized research methodology.

3. RESULTS, INTERPRETATION, AND DISCUSSION

A total of 23 species from 10 genera of calcareous nannofossils were determined (**Figure 5**) and presented in **Table 1, 2, and 3**. Moreover, foraminifera specimens in samples BK 78F and BK 95A were analysed using a semiquantitative method, to support the calcareous nannofossils data (**Table 4 and 5**).

3.1 Biostratigraphy

- Section BK 78

This section is located in the southern part of Supiori Island (**Figure 1**) and composed of Wainukendi Formation. There are three calcareous nannofossil zones identified on this section:

- *Discoaster deflandrei* Partial Range Zone: marked by *Discoaster deflandrei*' Last Occurrence (LO) at the top, with undefined bottom border. *Sphenolithus neoabies* occurs at the lowest interval suggesting equivalency with NN7 (Middle Miocene), which is also supported by semiquantitative foraminifera analysis results of BK 78F (N12 or Middle Miocene) (**Figure 6**).
- *Discoaster deflandrei* – *Discoaster neohamatus* Range Zone: marked by *Discoaster deflandrei*' LO (bottom) and *Discoaster neohamatus'* First Occurrence (FO) (top), and coeval with NN8 (Middle Miocene).
- *Discoaster neoha*matus Partial Range Zone: marked by *Discoaster neohamatus*' FO at the bottom with undefined top border. *Discoaster hamatus* occurs at the youngest interval suggesting equivalency with NN9 (Middle Miocene)

- Section BK 98

This section is located at the northern part of Supiori Island (**Figure 1**) and composed of Wafordori Formation. Based on calcareous nannofossils biozonation, this section is confirmed to be coeval with NN7 (Middle Miocene), which marked by the occurrence of *Discoaster kugleri*.

- Section BK 95

This section is located approximately 5 km westward of the BK 98 section (**Figure 1**) and composed of Napisendi Formation with four calcareous nannofossil zones:

- *Discoaster formosus* Partial Range Zone: marked by *Discoaster formosus'* LO at the top with undefined bottom border. *Discoaster moorei* occurrences at the lowest interval suggest NN5 (Middle Miocene) age, which supported by semiquantitative foraminifera analysis results on BK 95A sample (N11 or Middle Miocene).

DOI: 10.5614/bull.geol.2019.3.3.4

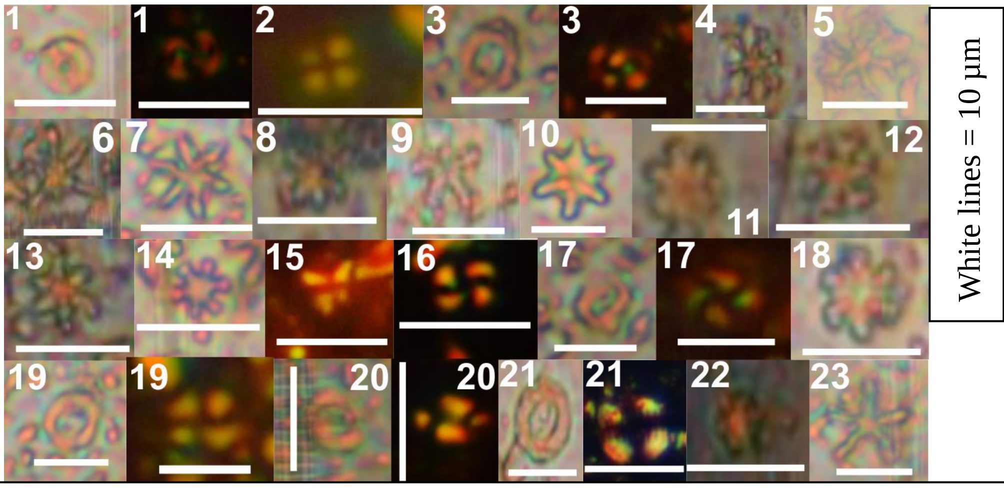

(1) *Calcidiscus leptoporus* ; (2) *Sphenolithus abies* ;(3) *Helicosphaera carteri* ; (4) *Discoaster variabilis*; (5) *Discoaster signus* ; (6) *Discoaster petaliformis* ; (7) *Discoaster neohamatus* ; (8) *Discoaster musicus* ; (9) *Discoaster moorei*. ; (10) *Discoaster kugleri* ; (11) *Discoaster druggi* ; (12) *Discoaster deflandrei* ; (13) *Discoaster formosus* ; (14) *Discoaster bolii* ; (15) *Sphenolithus heteromorphus* ; (16) *Reticulofenestra haqii* ; (17) *Helicosphaera obliqua* ; (18) *Discoaster calculosus*. (19) *Helicosphaera mediterranea* ; (20) *Helicosphaera ampliaperta* ; (21) *Coccolithus pelagicus* ; (22) *Catinaster coalitus extensus*; (23) *Discoaster hamatus*

Figure 5. Identified calcareous nannofossils taxa.

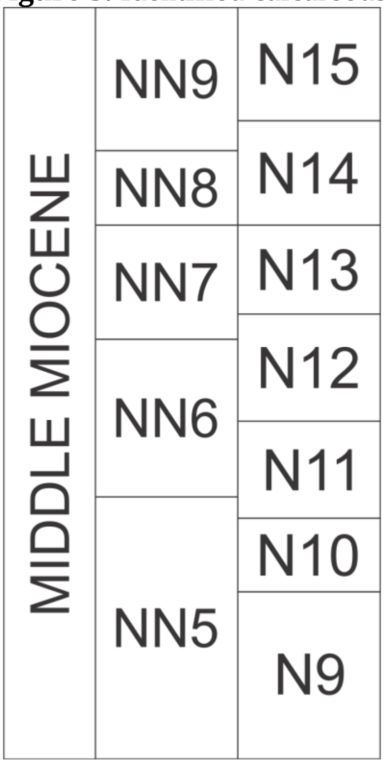

Figure 6. Correlation between calcareous nannoplankton zonation (NN) by Martini (1971) and planktonic zonation (N) by Blow (1969) (Martini, 1971).

- *Discoaster formosus–Discoaster kugleri* Range Zone: marked by *Discoaster formosus'* LO (bottom) and *Discoaster kugleri'* FO (top) that coeval with NN6 (Middle Miocene).
- *Discoaster kugleri* Interval Zone: marked by the occurrences of *Discoaster kugleri* that coeval with NN7 (Middle Miocene).
- *Discoaster kugleri – Discoaster hamatus* Range Zone: marked by *Discoaster kugleri'* LO (bottom) and *Discoaster hamatus'* FO (top), coeval with NN8 (Middle Miocene).
- *Discoaster hamatus* Partial Range Zone: marked by *Discoaster hamatus'* FO at the bottom with an undefined top border, however it can be concluded that this zone coeval with NN9 (Middle Miocene) as *Discoaster hamatus* is the fossil index for NN9 (Martini, 1971).

DOI: 10.5614/bull.geol.2019.3.3.4

Table 1. Calcareous Nannofossils Chart of BK 98

Age	Neogene Calcareous Nannofossils Zonation (Martini, 1971)	Formation	Unit	Biostratigraphic Comments	Sample	Abundance Estimation	Calcareous Nannofossils: *Discoaster deflandrei* (-NN7)	*Discoaster moorei* (NN5-NN7)	*Discoaster variabilis* (NN4-N16)	*Discoaster* spp.	*Discoaster druggi* ? (NN2-NN3)	*Discoaster kugleri* (NN7)	*Calcidiscus leptoporus* (NN2-Recent)	*Calcidiscus macintyrei* (NN4-NN19)	*Helicosphaera mediterranea* (NN2-NN7)	*Coccolithus pelagicus* (NP2-Recent)	*Helicosphaera carteri* (NN1-Recent)	*Reticulofenestra minuta* (NP13-Pliosen)	*Sphenolithus neoabies* (NN7-NN15)	*Discoaster exilis* (NN5-NN8)	*Reticulofenestra haqii* (NN2-NN15)	*Helicosphaera scissura* (NN3-NN4)	*Sphenolithus heteromorphus* (NN3-NN5)	*Helicosphaera* spp.	*Reticulofenestra pseudoumbilicus* (NN4-NN15)	*Cyclicargolithus floridanus* (-NN6)	*Discoaster challengeri* (NN7-NN15)
Middle Miocene	NN7	Wafordori	Calcareous Sandstone - Claystone	*Discoaster kugleri* →	BK 98C	A	320	80	80	80	1	80	80	80	80	240	80	240	320								
					BK 98B	A				80				240	80	80	80	80	320	240	160	1	1				
				Discoaster kugleri →	BK 98A	A	840	120				120	120			120	120	720	240		160		1	120	120	2	240

→ Occurrence A : Abundant

Table 2. Calcareous Nannofossils Chart of BK 78

Age	Neogene Calcareous Nannofossils Zonation (Martini, 1971)	Formation	Unit	Biostratigraphic Comments	Sample	Abundance Estimation	Calcareous Nannofossils: *Helicosphaera carteri* (NN1-Recent)	*Helicosphaera mediterranea* (NN2-NN7)	*Calcidiscus leptoporus* (NN2-Recent)	*Discoaster* spp.	*Discoaster hamatus* (NN9)	*Discoaster deflandrei* (-NN7)	*Discoaster neohamatus* (NN9-NN11)	*Discoaster challengeri* (NN5-NN10)	*Sphenolithus neoabies* (NN7-NN15)	*Chiasmolithus* spp.	*Helicosphaera oblique* (-NN6)	*Reticulofenestra haqii* (NN2-NN15)	*Helicosphaera ampliaperta* (NN2-NN4)	*Sphenolithus heteromorphus* (-NN4)	*Coccolithus pelagicus* (NP2-Recent)	*Discoaster signus* (NN6-NN7)	*Discoaster musicus* (NN5-NN6)	*Discoaster formosus* (NN5)	*Sphenolithus radians* (NP14-NP20)	*Helicosphaera scissura* (NN3-NN4)	*Cyclicargolithus floridanus* (-NN6)	*Discoaster druggi* (NN2-NN3)	*Discoaster exilis* (NN5-NN8)	*Marthasterites bramlettei* (NP10)	*Reticulofenestra minuta* (NP13-NN18)	*Discoaster moorei* (NN5-NN7)	*Discoaster braarudi* (NN6-NN10)
Middle Miocene	NN9	Wainukendi	Limestone - Calcareous Siltstone	*Discoaster hamatus* → (Occurrence)	BK 78A	F	120	1	20	20	20	1	40	20																			
				Discoaster neohamatus (FO)	BK 78B	F	280	1	40	40	40	2	40	40	40																		
	NN8				BK 78C	F	180	3		40		1		40		1	2	20	1	1	20												
					BK 78D	F	80	1	20					20			1				40		1										
	NN7			*Discoaster deflandrei* (LO)	BK 78E	C	80	80	80	320		240		160	720	2			4	2	80	80		2	1	1	1	1	80	1	320		
				Sphenolithus neoabies → (Occurrence)	BK 78F	C	80					240		480	1360			160		2	80	80		1				1	80	1	400	160	80

First Occurence (FO) Last Occurence (LO) → Occurrence C : Common F : Few

DOI: 10.5614/bull.geol.2019.3.3.4

Table 3. Calcareous Nannofossils Chart of BK 95

Age	Neogene Calcareous Nannofossils Zonation (Martini, 1971)	Formation	Unit	Biostratigraphic Comments	Sample	Calcareous Nannofossils																																						
						Abundance Estimation	*Calcidiscus leptoporus* (NN2-Recent)	*Helicosphaera carteri* (NN1-Recent)	*Helicosphaera mediterranea* (NN2-NN7)	*Helicosphaera oblique* (-NN6)	Coccolithus biparteoperculatus	*Discoaster brouweri* (NN8-NN18)	*Discoaster bolii* (NN8-NN10)	*Discoaster challengeri* (NN5-NN10)	Discoaster deflandrei (-NN7)	*Discoaster hamatus* (NN9)	*Discoaster exilis* (NN5-NN8)	*Discoaster formosus* (NN5)	*Discoaster calculosus* (-NN7)	*Reticulofenestra haqii* (NN2-NN15)	*Marthasteriter* sp. ?	*Discoaster kugleri* (NN7)	Coccolithus pelagicus (NP2-Recent)	*Discoaster* spp.	*Reticulofenestra minuta* (NN13-NN18)	*Reticulofenestra pseudoumbilicus* (NN4-NN15)	*Sphenolithus neoabies* (NN7 - NN15)	*Helicosphaera scissura* (NN1-NN4)	*Cruciplacolithus* spp.	*Coccolithus formosus* (NP12-NP21)	*Catinaster coalitus* (NN8-NN9)	*Discoaster braarudi* (NN6-NN10)	*Helicosphaera ampliaperta* (NN2-NN4)	*Discoaster moorei* (NN5-NN7)	*Chiasmolithus* spp. ?	*Cyclicargolithus floridanus* (-NN6)	*Sphenolithus radians* (NP11-NP19)	*Discoaster saipanensis* (NP14-NP20)	*Discoaster musicus* (NN5-NN6)	*Sphenolithus heteromorphus* (NN3-NN5)	*Discoaster druggi* (NN2-NN3)	*Rhabdosphaera* spp.	*Discoaster petaliformis* (NN4-NN5)	*Coccolithus* sp.
Middle Miocene	NN9	Napisendi	Calcareous Sandstone - Siltstone	*Discoaster hamatus*	BK 95K	C	840	2040	1	1	1	120	120	120	1	120																												
	NN8				BK 95J	C	600	1440	1	1	1		120	120			120	2	1	120	1																							
	NN7			*Discoaster kugleri*	BK 95I	A	480	240	240					120	480		480			240		240	480	1200	2400	240	240	2	4	2	2	240												
					BK 95H	A	120	360	120					360	240		120	1		480		120	120	480	1560	480	360				1													
					BK 95G	A	360	120		1				240	120		120	1				120	240	120	960	360	120						1	120	120									
					BK 95F	A	160	160		2				560			160			960				240	240			2				560				1	2	1						
				Discoaster kugleri	BK 95E	A	160	80	160								80			80		240	240	320		320	160						2	80										
	NN6				BK 95D	A	80	160						480	80			2		80			80		80		1					320							80	1				
					BK 95C	A	360	240	240					480	240		120			120					840		1						1			240				2	1	1		
	NN5			*Discoaster formosus*	BK 95B	A	120	120		240				240	240		480	240			1		240		600								2			360	1			1	2		120	
				Discoaster moorei	BK 95A	A	600	240	120	120				480	120		120	480					240		360			1						120		120				120	1			1

First Occurence (FO) Last Occurence (LO) Occurrence A : Abundant C : Common

Table 4. Semiquantitative Analysis of Foraminifera on BK 78F

Num.	Planktonic Foraminifera	Abundance	Age (Blow, 1969, 1970)																		
			N4	N5	N6	N7	N8	N9	N10	N11	N12	N13	N14	N15	N16	N17	N18	N19	N20	N21	N22
1	*Globigerinoides trilobus immaturus*	Common																			
2	*Globigerinoides trilobus saccuiferus*	Few																			
3	*Orbulina universa*	Abundant																			
4	*Globigerinoides trilobus trilobus*	Comon																			
5	*Biorbulina bilobata*	Few																			
6	*Hastigerina siphonifera*	Few																			
7	*Globigerinoides obliquus*	Common																			
8	*Globoquadrina altispira*	Common																			
9	*Globorotalia mayeri*	Common																			
10	*Globigerina venezuelana*	Common																			
11	*Globorotalia siakensis*	Abundant																			
12	*Globorotalia obesa*	Few																			
13	*Sphaeroidinellopsis seminulina seminulina*	Few																			
14	*Globorotalia fohsi fohsi*	Few																			
15	*Globorotalia praemenardii*	Rare																			
16	*Globoquadrina dehiscens*	Common																			
17	*Globorotalia fohsi robusta*	Few																			

AGE **: N12**

Num.	Benthonic Foraminifera Association	Abundance
1	*Bolivinita quadrilatera*	Few
2	*Bolivina* spp.	Few
3	*Globocassidulina subglobosa*	Few
4	*Planulina bradyii*	Rare

Abundant : >25 specimens
Common : 11 - 25 specimens
Few : 4 - 10 specimens
Rare : 1 - 3 specimens

DEPOSITIONAL ENVIRONMENT:
Bathyal (Boltovskoy and Wright, 1976; Murray, 2006)

Table 5. Semiquantitative Analysis of Foraminifera on BK 95A

Num.	Planktonic Foraminifera	Abundance	Age (Blow, 1969, 1970)																		
			N4	N5	N6	N7	N8	N9	N10	N11	N12	N13	N14	N15	N16	N17	N18	N19	N20	N21	N22
1	*Globigerinoides trilobus immaturus*	Common																			
2	*Globigerinoides trilobus saccuiferus*	Few																			
3	*Orbulina universa*	Abundant																			
4	*Globigerinoides trilobus trilobus*	Common																			
5	*Biorbulina bilobata*	Few																			
6	*Globigerinoides obliquus*	Common																			
7	*Globoquadrina altispira*	Common																			
8	*Globorotalia mayeri*	Common																			
9	*Globigerina venezuelana*	Common																			
10	*Globorotalia siakensis*	Abundant																			
11	*Globorotalia peripheroronda*	Few																			
12	*Sphaeroidinellopsis seminulina seminulina*	Few																			
13	*Globorotalia peripheroacuta*	Few																			
14	*Globorotalia praemenardii*	Rare																			
15	*Globoquadrina dehiscens*	Common																			
17	*Globorotalia scitula*	Few																			

AGE **: N11**

Abundant : >25 specimens
Common : 11 - 25 specimens
Few : 4 - 10 specimens
Rare : 1 - 3 specimens

Num.	Benthonic Foraminifera Association	Abundance
1	*Bolivinita quadrilatera*	Rare
2	*Bolivina* spp.	Rare
3	*Globocassidulina subglobosa*	Rare
4	*Planulina bradyii*	Rare
5	*Laticarinina pauperata*	Rare
6	*Amphistegina lessonii*	Rare
7	*Siphonina* sp.	Rare
8	*Lenticulina* sp.	Rare
9	*Stilostomella* spp.	Few
10	*Nodosaria* spp.	Rare
11	*Pullenia* sp.	Rare
12	*Gyroidina soldanii*	Few
13	*Sphaerodina bulloides*	Few
14	*Siphongenerina* spp.	Rare
15	*Pleurostomella* spp.	Few

DEPOSITIONAL ENVIRONMENT:
Bathyal (Boltovskoy and Wright, 1976; Murray, 2006)

DOI: 10.5614/bull.geol.2019.3.3.4

3.2 Thermocline/Nutricline Depth

Thermocline is oceanic water layer in which water temperature decreases rapidly with increasing depth, while nutricline is an ocean layer in which there is a high variation of nutrient content, their depth is very close to each other under every condition hence generally associable (Bown et al., 2004). In this research, relatively high *Discoaster* abundance (>=20 %) and large coccolith size (>=3 μm) indicate a deep thermocline/nutricline depth (oligotrophic condition), while relatively low *Discoaster* abundance (<20%) and small coccolith size (<3 μm) represent thermocline/nutricline shoaling (eutrophic condition).

- Section BK 78

Mean coccolith size measurements show an increasing trend from BK 78F (~3μm) to BK 78C (~5μm), while *Discoaster* abundance generally decrease from BK 78F (~33%) to BK 78D (~15%) and then gradually increase towards BK 78A (~35%) (**Figure 7a**). These results indicate an initial oligotrophic condition during NN7, before the significant change to eutrophic conditions since early NN8 and then gradually shifted back to oligotrophic conditions since late NN8. In this section, the last thermocline/nutricline shifting (late NN8–NN9) from eutrophic to oligotrophic is inferred from *Discoaster* abundance due to the absence of *Reticulofenestra* and *Coccolithus* at the two youngest samples. Their absence could be related to ecological or preservation factor, however it wasn't analysed in this research.

- Section BK 95

In general, mean coccolith size measurements show a slight decreasing trend from BK 95A (~5μm) to BK 95I (~3,5μm) and genera of *Reticulofenestra* and *Coccolithus* are absent from BK 95J to BK 95K. In addition, *Discoaster* abundance also denotes a slightly declining trend from BK 95A (~40%) to BK 95C (~30%), before a drastic decrease between BK 95B and BK 95A (~10%) (**Figure 7b**). Those parameters indicates a relatively oligotrophic depositional condition during NN5– NN7, which then significantly shifted to the eutrophic condition since NN8.

3.3 Paleosalinity

Paleosalinity conditions are inferred from the abundance of *Helicosphaera carteri*, *Calcidiscus leptoporus*, and *Sphenolithus neoabies* (modified from Santoso et al., 2014). *Helicosphaera carteri* and *Calcidiscus leptoporus* are abundant in hyposaline condition (Melinte, 2004; Wade and Brown, 2006 in Santoso et al., 2014), while *Sphenolithus abies* are highly abundant in sediments deposited under normal saline condition (Wade and Brown, 2006 in Santoso et al., 2014). In this research, *Sphenolithus neoabies* were used as normal saline parameters instead of *Sphenolithus abies* due to the later absence. *Sphenolithus neoabies is* generally associated with *Sphenolithus abies* in the Upper Tertiary sediments (Towe, 1979) and considered as small variants of *Sphenolithus abies* (Bukry and Bramlette, 1969). In this research, paleosalinity analysis was only conducted from NN7–younger sediment interval due to the absence of *Sphenolithus neoabies* at the lower interval (NN5–NN6/early Middle Miocene).

- Section BK 78

In BK 78F–BK 78E interval (NN7), *Sphenolithus neoabies* has a relatively high abundance (~35–40%), while *Helicosphaera carteri* and *Calcidiscus leptoporus* occur in low abundance (<5%), indicating a normal saline condition. *Sphenolithus neoabies* abundances were drastically decline ~0–8 % in BK 78D–BK 78A (NN8–NN9/late Middle Miocene) interval, while *Helicosphaera carteri* became significantly abundant (~50–58%) and *Calcidiscus leptoporus* became slightly abundant (~10–13%), indicated paleosalinity shift from normal to hyposaline (**Figure 8a**).

- Section BK 95

BK 95E–BK 95I interval (NN7) show a relatively equal abundance of *Sphenolithus neoabies* (~0–8%), *Helicosphaera carteri* (~8%), and *Calcidiscus leptoporus* (~2–0%),

DOI: 10.5614/bull.geol.2019.3.3.4

in this case, paleosalinity level were assumed at normal saline. *Helicosphaera carteri* and *Calcidiscus leptoporus* abundance were drastically increase (~60% and ~25% respectively) on BK 95J–BK 95 K interval (NN8–NN9/late Middle Miocene), while *Sphenolithus neoabies* became absent, indicated a drastic changes to hyposaline condition (**Figure 8b**).

3.4 Discussion

Biostratigraphic analysis from section BK 78, BK 95, and BK 98 show biozonation range from NN5 to NN9, which coeval to Middle Miocene. These results corresponding to Pieters et al. (1983), which propose the Early–Middle Miocene Age for Napisendi and Wafordori Formation, as well as the Oligocene–Middle Miocene Age for Wainukendi Formation. Therefore, it can be concluded that these formations have a correlatable interval (NN7) and interfingering each other (**Figure 9**).

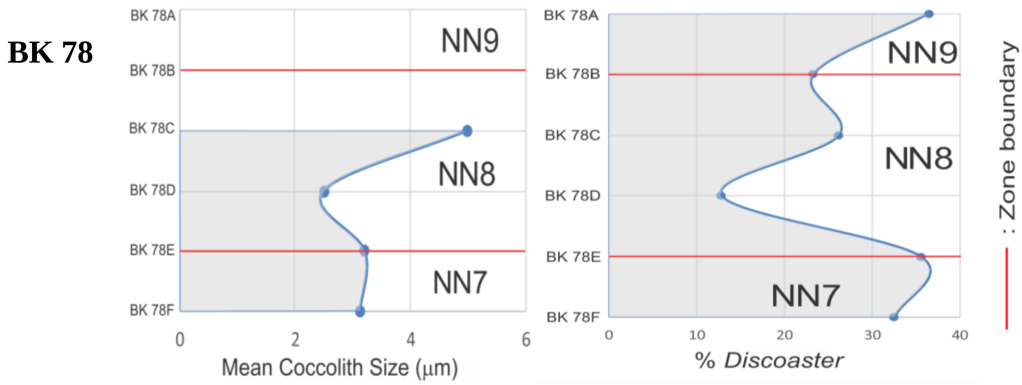

Figure 7a. Mean coccolith size (µm) of section BK 78 and BK 95.

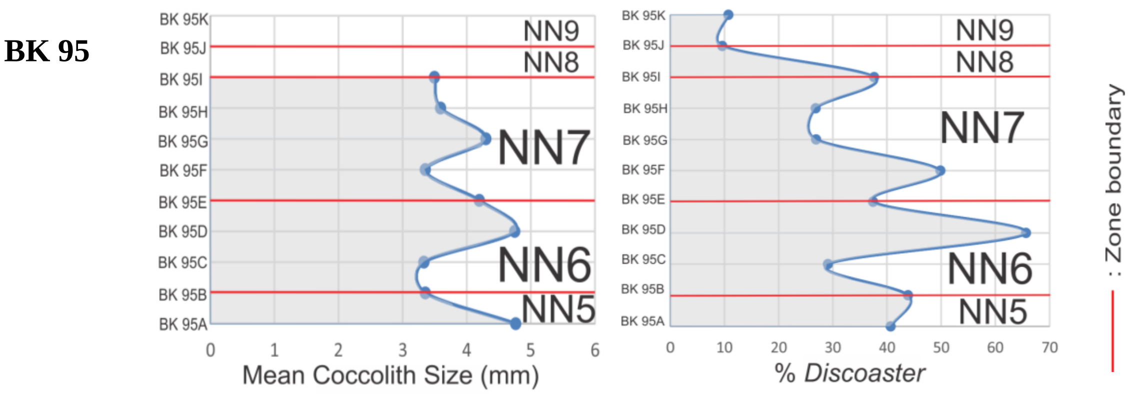

Figure 7b. *Discoaster* abundance of section BK 78 and BK 95.

Paleoecological analyses on thermocline/nutricline depths showed a rather fluctuating result during Middle Miocene (NN5–NN9), which changed from oligotrophic (NN5–NN7/early Middle Miocene) to eutrophic (Early NN8), and back to oligotrophic (Late NN8–NN9/late Middle Miocene). These conditions probably related to the pre-closure condition of Indonesian and Central American Seaways during Middle Miocene which allowed intermediate waters from Pacific Ocean flowed freely to Indian Ocean causing changes on thermocline/nutricline depth at Western Equatorial Pacific (Kennett, et al., 1985; Duque-Caro, 1990; Droxler, et al., 1998 in Nathan and Leckie, 2009). The closure of Indonesian Seaways was caused by regional uplift, which involved the complex tectonic movement of Banda Arc, Borneo, and Papua (Hodel and Vayavananda, 1993). Similar cases also happened at Central American Seaway

DOI: 10.5614/bull.geol.2019.3.3.4

(Haug, et al., 2001; Steph, et al., 2006; Kamikuri, et al., 2009 in Rouselle, et al., 2013). Both closures took place roughly at 20–10 million years ago (ma) or during the late Middle–early Late Miocene (Moberly, 1972; Audley-Charles, et al., 1972; Edwards, 1975; Hamilton, 1979 in Hodel and Vayavananda, 1993), which caused a reorganization of sea surface circulation on Equatorial Pacific (Edwards, 1975; Kennett, et al., 1985 in Hodell dan Vayavananda, 1993). The thermocline/nutricline deepening, since the late NN8 (late Middle Miocene), might be related to the narrower Indonesian Seaway, which caused the formation of proto WPWP (Nathan and Leckie, 2009). Furthermore, an Equatorial Under Current (EUC), which draw off nutrition eastward, also formed and caused a deeper thermocline/nutricline at the Equatorial Western Pacific (Nathan and Leckie, 2009). However, more accurate methods are needed to know the detailed thermocline/nutricline depth between the earlier and later oligotrophic phases.

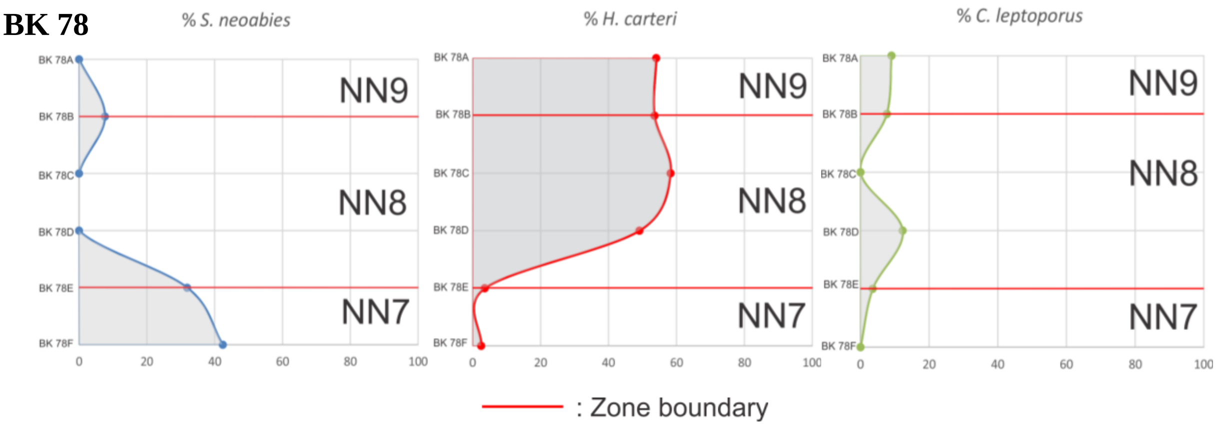

Figure 8a. Abundance percentages of *Sphenolithus neoabies*, *Helicosphaera carteri*, and *Calcidiscus leptoporus* on section BK 78.

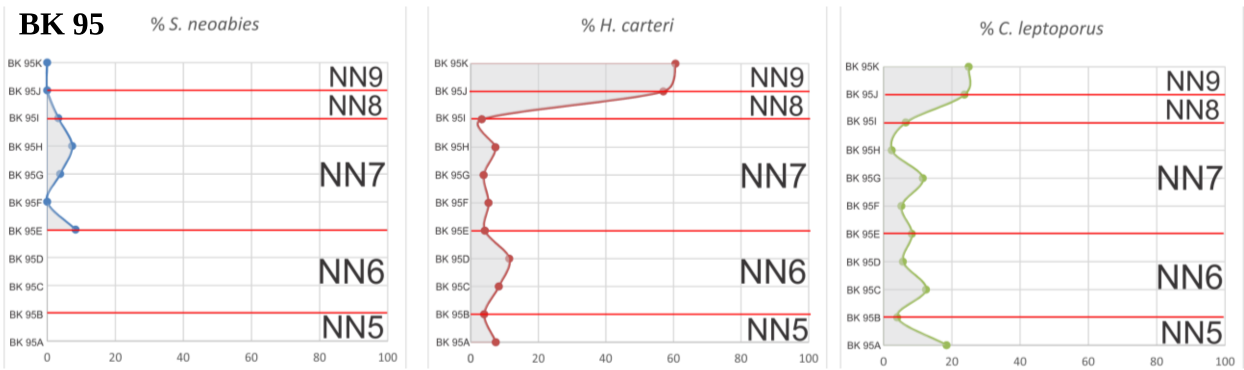

Figure 8b. Abundance percentages of *Sphenolithus neoabies*, *Helicosphaera carteri*, and *Calcidiscus leptoporus* on section BK 95.

Paleosalinity parameters indicate a shift from normal saline in NN7 to a hyposaline condition in NN8–NN9 (late Middle Miocene) Zone. Salinity decline during late Middle–early Late Miocene is also suggested by Rouselle et al. (2013) based on $\delta^{18}O$ measurements of *Noelarhabdoceae* nannofossils at IODP U1338 site, Eastern Equatorial Pacific. That change might also correspond with the gradual closure of Indonesian and Central American Seaways, which made it narrower (Haug, et al., 2011; Molnar and Cane, 2002; Gussone, et al., 2004 in Rouselle, et al., 2013). These closures caused the formation of proto WPWP, which triggered a *La Nina*-like conditions (Nathan and Leckie, 2009). As a result, the Western

DOI: 10.5614/bull.geol.2019.3.3.4

Equatorial Pacific, including Indonesian Archipelago, underwent high precipitation, which might correspond to the paleosalinity shift during late Middle Miocene (NN8– NN9). This paleosalinity shift inferred the possibility of proto WPWP formation at least on the late Middle Miocene. Paleo-oceanographic condition summary of the Supiori Island during Middle Miocene is presented in **Figure 10**.

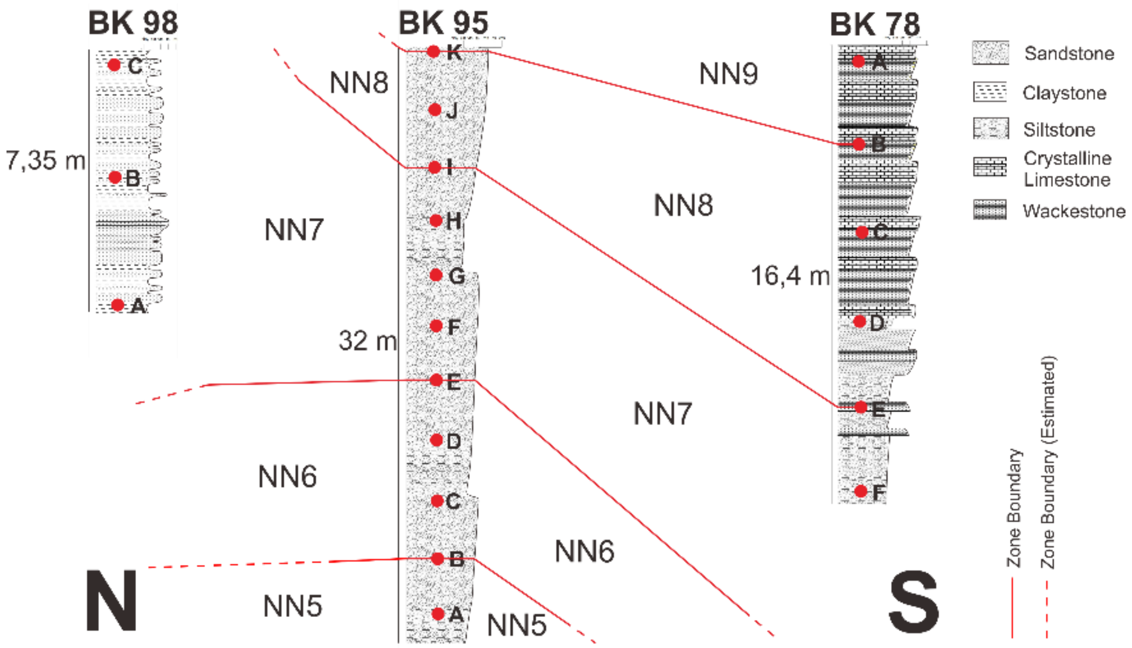

Figure 9. Biostratigraphic correlation of BK 98, BK 95, and BK 78 sections.

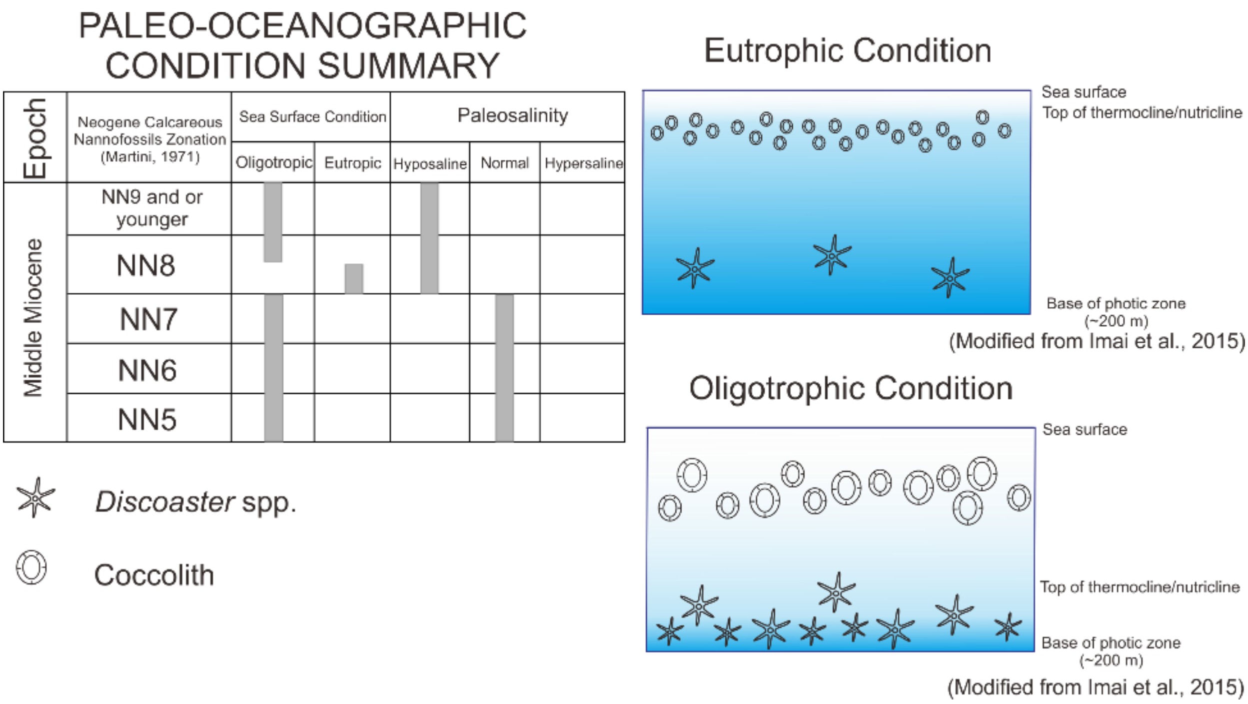

Figure 10. Paleo-oceanographic condition summary of Supiori Island during Middle Miocene.

DOI: 10.5614/bull.geol.2019.3.3.4

4. CONCLUSIONS

Based on the calcareous nannofossils zonation by Martini (1971), section BK 78 is categorised into three zones, which coeval to NN7–NN9, section BK 95 is categorised into five zones, which coeval to NN5–NN9, and section BK 98 considered as equivalent to NN7. These results show a correlatable interval between Wafordori, Napisendi, and Wainukendi Formation (NN7), which indicate an interfingering contact between these formations.

Thermocline/nutricline depth analyses from *Discoaster* abundance and the mean coccolith size of *Reticulofenestra* and *Coccolithus* indicate sea surface condition changes from oligotrophic (NN5–NN7/early Middle Miocene) to eutrophic (early NN8), then back to oligotrophic (late NN8–NN9/late Middle Miocene). Those changes related to the closure of Indonesian Seaways, which triggered the formation of proto WPWP and EUC causing a deeper thermocline/nutricline since late Middle Miocene (late NN8–NN9). More accurate methods are needed to know the detailed thermocline/nutricline depth between the earlier (NN5–NN7/early Middle Miocene) and later (after late NN8/late Middle Miocene) oligotrophic phases.

Paleosalinity analysis, based on abundance comparison between *Sphenolithus neoabies*, *Helicosphaera carteri*, and *Calcidiscus leptoporus* show paleosalinity shift from normal saline (NN7) to hyposaline conditions (NN8–NN9 and or younger). The paleosalinity shift corresponded to the possible formation of proto WPWP, at least in the Late Middle Miocene. The formation of proto WPWP triggered a *La Nina*-like condition since late Middle Miocene (NN8–NN9 and/or younger) causing high precipitation at Indonesian Archipelago.

ACKNOWLEDGMENT

We would like to express our deepest gratitude to Geological Research Centre for providing the research materials, Rudy Lesmana, S.T. in Micropaleontology Laboratory ITB for samples preparation, and our colleagues in Geological Engineering Graduates Program of ITB for the supports.

REFERENCES

Alviyanda, Junursyah, G.M., Saragih, R. 2019. Reservoir Potential of Neogene Rocks in The Biak Island and Its Surrounding Areas. *Indonesian Journal of Sedimentary Geology*, 42, 33 – 41.

Audley-Charles, M.G., Carter, D.J. and Milsom, J.S., 1972. Tectonic development of Eastern Indonesia in relation to Gondwanaland dispersal. Nature Physical Science, 239, 35-39.

Berggren W.A., Kent D.V., Swisher III C.C., AUBRY M. P., 1995, A revised Cenozoic chronology and chronostratigraphy. *in* Berggren W.A., Kent D.V., Hardenbol, J. (Eds.), Geochronology, Time Scale and Global Stratigraphic Correlations. Framework for an Historical Geology. SEPM Special Publication, 54: 129 – 212.

Blow, W.H., 1969. Late Middle Eocene to Recent planktonic foraminiferal Biostratigraphy *in* Bronnimann, R. & Renz, H. H., 1969, ed., *Proceedings of the First International Conference on Planktonic Microfossils*, 1, 199 – 421, Geneva.

Blow, W.H., 1970. Validity of biostratigraphic correlations based on the Globigerinacea, *Micropaleontology*, 16, 257 – 268.

Boltovskoy, E. dan Wright, R., 1976: *Recent foraminifera*, Springer Science+Business Media B.V., Dordrecht, 95 – 274.

Bown, P., Lees, J.A., Young, J.R., 2004. Calcareous nannoplankton evolution and

DOI: 10.5614/bull.geol.2019.3.3.4

diversity through time. *in* Thierstein, H.R., Young, J.R., ed., Coccolithophores: From molecular processes to global impact. Springer-Verlag, New York, 481–508.

Bukry, D. and Bramlette, M.N., 1969. Some new and stratigraphically useful calcareous nannofossils of the Cenozoic, *Tulanes studies in Geology and Paleontology*, 7: 131 – 142.

Droxler, A., Burke, K., Cunningham, A., Hine, A., Rosencrantz, E., Duncan, D., Hallock, P., Robinson, E., 1998. Caribbean constraints on circulation between Atlantic and Pacific oceans over the past 40 million years. *in* Crowley, T., Burke, K., ed, Tectonic boundary conditions for climate reconstructions. Oxford University Press, Oxford, 169–191.

Duque-Caro, H., 1990. Neogene stratigraphy, paleoceanography and paleobiogeography in Northwest South America and the evolution of the Panama Seaway. Palaeogeography, Palaeoclimatology, Palaeoecology, 77(3–4), 203–234. doi:10.1016/0031-0182(90)90178-a

Edwards, A.R., 1975. Southwest Pacific Cenozoic palcogeography and an integrated Ncogene paleocirculation model. Initial Reports of DSDP, 30, 667-684.

Farida, M., Imai, R., and Sato, T., 2012. Miocene to Pliocene Paleoceanography of the Western Equatorial Pacific Ocean Based on Calcareous Nannofossils, ODP Hole 805B, *Open Journal of Geology*, **2**: 72 – 79. doi:10.4236/ojg.2012.22008

Gussone, N., Eisenhauer, A., Tiedemann, R., Haug, G. H., Heuser, A., Bock, B., Nagler, Th. F., Muller, A., 2004. Reconstruction of Carribean Seasurface temperature and salinity fluctuations in response to the Pliocene closure of the Central American Gateway and radiative forcing, using $\delta^{44/40}$Ca, δ^{18}O and Mg/Ca ratios. Earth Planetary Science Letters 227, 201–214.

Hamilton, W., 1979. Tectonics of the Indonesian Region. Geological Society of America Professional Papers, 1078, 345 pp.

Haug, G.H., Tiedemann, R., Zahn, R., Ravelo, A.C., 2001. Role of Panama uplift on oceanic freshwater balance. Geology 293, 20–210.

Hodell, D.A., and Vayavananda, A., 1993. Middle Miocene paleoceanography of the western equatorial Pacific (DSDP site 289) and the evolution of Globorotalia (Fohsella), *Marine Micropaleontology*, 22, Elsevier Science Publishers B. V., Amsterdam, 279-310.

Imai, R., Farida, R., Sato, T., and Iryu Y., 2015. Evidence for eutrophication in the Northwestern Pacific and Eastern Indian Oceans during the Miocene to Pleistocene based on the nannofossil accumulation rate, *Discoaster* abundance, and coccolith size distribution of *Reticulofenestra*, *Marine Micropaleontology*, 116, 15 – 27. doi:10.1016/j.marmicro.2015.01.001

Jatiningrum, R.S. and Sato, T., 2017. Sea-Surface Dynamics Changes in the Subpolar North Atlantic Ocean (IODP Site U1314) during Late Pliocene Climate Transition Based on Calcareous Nannofossil Observation, *Open Journal of Geology*, 10, 72 – 79. doi:10.4236/ojg.2017.710103

Junursyah, G.M.L., Saragih, R.Y., and Alviyanda, 2017. Biak – Numfor stratigraphy research final report, Geological Research Centre, Bandung (Unpublished).

Kamikuri, S., Motoyama, I., Nishi, H., Iwai, M., 2009. Evolution of Eastern Warm Pool and upwelling processes since the middle Miocene based on analysis of radiolarian assemblages: response to

Indonesian and Central American Seaways. *Palaeogeography, Palaeoclimatology, Palaeoecology* 280, 469–479. doi:10.1016/j.palaeo.2009.06.034

Kennett, J.P., Keller, G., Srinivasan, M., 1985. Miocene planktic foraminifer biogeography and paleoceanographic development of the Indo-Pacific region. *in* Kennett, J.P., ed., The Miocene Ocean: Paleoceanography and Biogeography. Memoir, vol. 163, Geological Society of America, Boulder, CO, 197–236.

Martinez, J. I, Taylor, L., De Deccker, P., dan Barrows, T., 1998: Planktonic foraminifera from the eastern Indian Ocean: distribution and ecology in relation to the Western Pacific Warm Pool (WPWP), *Marine Micropaleontology* 34, 121 – 151. doi:10.1016/s0377-8398(97)00045-5

Martini, E., 1971. Standard Tertiary and Quaternary calcareous nannoplankton zonation, *op cit.* Farinacci, A., ed., *Proceedings of the Second Planktonic Conference*, Roma, Tecnoscienza, 739–785.

Masria, M., Ratman, N., and Suwitodirdjo, K., 1981. Geology of the Biak Quadrangle, Irian Jaya, explanatory notes and Geological Map, 1:250,000 Scale, Biak Sheet, Quadrangle 3115, Geological Research and Development Center, Bandung.

McAdoo, R.L., and Haebig, J.C., 2000. Tectonic elements of the North Irian Basin, *Proceedings Indonesian Petroleum Association Twenty Seventh Annual Convention*, IPA, Jakarta, 150 – 166.

Melinte, M.C., 2004. Calcareous nannoplankton, a tool to assign enviromental changes, *Geo Eco Marina* 9–10, 9 pp. doi:10.5281/zenodo.57517

Moberly, R., 1972. Origin of lithosphere behind island arcs, with reference to the Western Pacific. *Geological Society of America Memoir* 132, 35-55.

Molnar, P., Cane, M.A., 2002. El Nino's tropical climate and teleconnections as a blueprint for pre-Ice Age climate. *Paleoceanography* 172, 1–13. doi:10.1029/2001pa000663

Murray, J.W., 2006. *Ecology and applications of benthic foraminifera*, University press, Cambridge, 200 – 426.

Nathan, S.A., and Leckie R.M., 2009. Early history of the Western Pacific warm pool during the Middle to Late Miocene (~13.2 – 5.8 Ma):role of sea – level change and implications for equatorial circulation, *Paleogeography, Paleoclimatology, Paleoecology* 274, 140 – 159. doi:10.1016/j.palaeo.2009.01.007

Pratiwi, S.D. and Sato, T., 2016. Reconstruction of Paleoceanography Significance in the Western Pacific and Atlantic Oceans during the Neogene Based on Calcareous Nannofossil Productivity and Size Variations, Related to the Global Tectonic Events, *Open Journal of Geology* 6, 931 - 943. doi:10.4236/ojg.2016.68070

Perch – Nielsen, K., 1985. Cenozoic calcareous nannofossils, *in* Bolli, H. M., Saunders, J. B. and Perch – Nielsen, K., ed., *Plankton Stratigraphy*, Cambridge University Press, Cambridge: 428 - 484.

Permana, A. K., 2015. Biak – Yapen Basin stratigraphy research final report, Geological Research Centre, Bandung (Unpublished).

Pertamina (1999), Indonesia Gas Reserves and Resources Map, 1:5,000,000 scale, Pertamina, Jakarta.

Pieters, P. E., Pigram, C. J., Trail, D. S., Dow, D. B., Ratman, N., and Sukamto, R., 1983. The Stratigraphy of Western Irian Jaya, *Proceedings Indonesian Petroleum*

DOI: 10.5614/bull.geol.2019.3.3.4

Association Twelfth Annual Convention, 231 – 261.
Rousselle, G., Beltran, C., Sicre, M. A., Raffi, I., and Rafelis, M. D., 2013. Changes in sea-surface conditions in the Equatorial Pacific during the Middle Miocene – Pliocene as inferred from coccolith geochemistry, *Earth and Planetary Science Letters* 361, 412 – 421. doi:10.1016/j.epsl.2012.11.003
Sagawa, T., Yokoyama, Y., Ikehara, M., and Kuwae, M., 2012. Shoaling of the western equatorial Pacific thermocline during the last glacial maximum inferred from multispecies temperature reconstruction of planktonic foraminifera, *Paleogeography, Paleoclimatology, Paleoecology* 346–347, 120–129. doi:10.1016/j.palaeo.2012.06.002
Santoso, W. D., Insani, H., and Kapid, R., 2014. Paleosalinity conditions on Late Miocene – Pleistocene in the North East Java Basin, Indonesia based on nannoplankton population changes, *Riset Geologi dan Pertambangan* 24, 1 – 11. doi:10.14203/risetgeotam2014.v24.77
Steinke, S., Prange, M., Feist, C., Groeneveld, J., and Mohtadi, M., 2014. Upwelling variability off southern Indonesia over the past two millennia, *Geophysical Research Letter* 41, 7684 – 7693. doi: 10.1002/2014GL061450
Steph, S.,Tiedemann, R., Groeneveld, J.,Sturm,A., Nurnberg, D., 2006. Pliocene changes in Tropical East Pacific upper ocean stratification: response to tropical gateways? *in* Proceedings of the Ocean Drilling Program, *Scientific Results* 202, 1–51. doi:10.2973/odp.proc.sr.202.211.2006
Towe, K. M., 1979. Variation and systematics in calcareous nannofossils of the genus Sphenolithus. *American Zoologist* 19(2), *555 – 572*. doi:10.1093/icb/19.2.555
Wade, S.B. and Brown, R.P., 2006. Calcareous Nannofossils in Extreme Environments: The Messinian Salinity Crisis, Polemi Basin, Cyprus, *Palaeogeography, Palaeoclimatology. Palaeoecology* 233, 271–286. doi:10.1016/j.palaeo.2005.10.007
Waschsmuth, W. and Kunst, F. (1986). Wrench Fault tectonics in Northern Irian Jaya, *Proceedings of Indonesian Petroleum Association Eleventh Annual Convention*, IPA, Jakarta, 371–376.

DOI: 10.5614/bull.geol.2019.3.3.4